Inverse problem for the identification of Chaos representations of random fields using experimental vibrational tests

Christophe Desceliers, Christian Soize, R. Ghanem

Inverse problem for the identification of Chaos representations of random fields using experimental vibrational tests

C. Desceliers[a], **C. Soize**[a], **R. Ghanem**[b]
[a] University of Marne-la-vallée, Paris, France
[b] University of Southern California, United States of America
e-mail: **christophe.desceliers@univ-mlv.fr**

Abstract

This paper deals with the experimental identification of the probabilistic representation of a random field modeling the Young modulus of a non homogeneous isotropic elastic medium by experimental vibration tests. The random field representation is based on the polynomial chaos decomposition. The coefficients of the polynomial chaos are identified setting an inverse problem and then in solving an optimization problem related to the maximum likelihood principle.

1 Introduction

We consider an elastic isotropic heterogeneous material at the macroscopic scale. In this paper, this material is modeled by a random medium. Only the Young modulus is modeled by a random field. This random field has to be identified by using an experimental database constituted of vibrational tests related to 100 specimens in the frequency band [0-50]kHz. There are 60 sensors measuring accelerations. All the specimens are excited by the same loads whose spectrum are constant on the frequency band of analysis. The linear elastodynamics of the specimen is modeled by the finite element method. A chaos representation (see for instance [1, 2, 3]) of the random field modeling the Young modulus is introduced. This identification problem has been adressed in a recent work proposed in [4, 5]. The proposed method in [5] consists in identifying the coefficients of the chaos representation by using the experimental database related to the dynamical response of the specimen. The coefficients related to the finite element model of the specimen are random variables. The first step of the method consists in identifying the related realizations of these random variables by setting an optimization problem for each specimen. This optimization problem consists in minimizing the distance between the frequency responce functions of the database and the frequency response function of the finite element model with respect to the finite element coefficients of each specimen. In the second step of the method, the polynomial chaos representation of these random variables is introduced. In the last step of the method, the coefficients of the polynomial chaos representations are estimated by using the maximum likelihood method. A numerical example is presented in order to validate the methodology. The example consists in a viscoelastic random medium occupying a slender geometry. The experimental database is constructed by Monte Carlo numerical simulations of the direct problem. On the presented example, not only the autocorrelation functions of the random field can be identified, but also the first order marginal probability density functions.

2 Construction of an "experimental database" by Monte Carlo numerical simulation of the direct problem

In this paper, the “experimental database” is constructed by numerical simulation. The specimen is constituted of a non-homogeneous isotropic linear elastic medium occupying a three-dimensional bounded domain $\mathcal{D}$ with boundary $\partial\mathcal{D}$ given in a Cartesian system $Ox_1x_2x_3$. The geometry of domain $\mathcal{D}$ is a slender rectangular box shown in Fig. 1 whose dimensions along x_1, x_2 and x_3 are $L_1 = 1.3 \times 10^{-1}m$, $L_2 = 2 \times 10^{-2}m$ and $L_3 = 2 \times 10^{-2}m$. The structure is fixed on the part Γ_0 of $\partial\mathcal{D}$ for which the displacement field is zero.

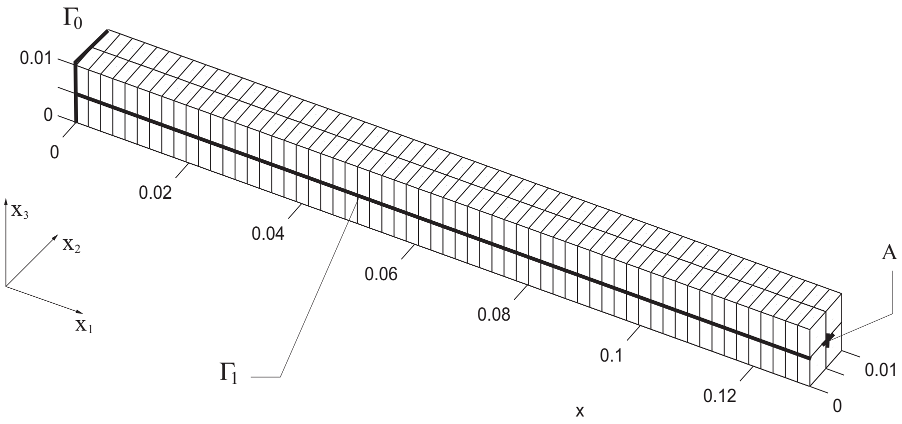

Figure 1: Definition of the specimen

The structure is subjected to an external point force denoted as $\mathbf{b}(t)$ and applied to the node A along x_1-axis (see Fig. 1). The Fourier transform $\widehat{\mathbf{b}}$ of $\mathbf{b}$ is the constant vector $(1, 0, 0)$ in the frequency band $[0, 50]$ kHz. The elastic medium is random. It is assumed that the Young modulus is random while the Poisson coefficient is deterministic. This assumption is introduced in order to simplify the presentation. The random Young modulus field is modeled by a positive-valued second-order random field $Y(\mathbf{x})$ defined by

$$Y(\mathbf{x}) = c_0\, g(c_1, c_2\, V(\mathbf{x})) \quad , \quad \forall \mathbf{x} \in \mathcal{D} \tag{1}$$

in which $c_0 = 1.6663 \times 10^{10}\ N.m^{-2}$, $c_1 = 1.5625$ and $c_2 = 0.2$. The function $\theta \mapsto g(\alpha, \theta)$ from $\mathbb{R}$ into $]0\,, +\infty[$ is such that, for all θ in $\mathbb{R}$,

$$g(\alpha, \theta) = F_{\Gamma_\alpha}^{-1}(F_\Theta(\theta)) \quad ,$$

in which $\theta \mapsto F_\Theta(\theta) = P(\Theta \leq \theta)$ is the cumulative distribution function of the normalized Gaussian random variable Θ and where the function $p \mapsto F_{\Gamma_\alpha}^{-1}(p)$ from $]0\,, 1[$ into $]0\,, +\infty[$ is the reciprocal function of the cumulative distribution function $\gamma \mapsto F_{\Gamma_\alpha}(\gamma) = P(\Gamma_\alpha \leq \gamma))$ of the gamma random variable Γ_α with parameter α. In the right-hand side of Eq. (1) , $\{V(\mathbf{x}), \mathbf{x} \in \mathcal{D}\}$ is a second-order random field such that $E\{V(\mathbf{x})\} = 0$ and $E\{V(\mathbf{x})^2\} = 1$, defined by

$$V(\mathbf{x}) = \sum_{|\boldsymbol{\alpha}|=1}^{3} H_{\boldsymbol{\alpha}}(Z_1, Z_2, Z_3, Z_4)\, \sqrt{\gamma_{\boldsymbol{\alpha}}}\, \psi_{\boldsymbol{\alpha}}(\mathbf{x}/2) \quad , \tag{2}$$

in which $\{Z_1, Z_2, Z_3, Z_4\}$ are independent normalized Gaussian random variables, $\boldsymbol{\alpha}$ is a multi-index $(\alpha_1, \alpha_2, \alpha_3, \alpha_4) \in \mathbb{N}^4$, $|\boldsymbol{\alpha}| = \alpha_1 + \alpha_2 + \alpha_3 + \alpha_4$ and where $H_{\boldsymbol{\alpha}}(z_1, z_2, z_3, z_4) = H_{\alpha_1}(z_1) \times H_{\alpha_2}(z_2) \times$

$H_{\alpha_3}(z_3) \times H_{\alpha_4}(z_4)$ in which $H_{\alpha_k}(z_k)$ is the normalized Hermite polynomial of order α_k such that

$$\int_{\mathbb{R}} H_{\alpha_k}(w)\, H_{\alpha_j}(w) \frac{1}{\sqrt{2\pi}} e^{-\frac{1}{2}w^2}\, dw = \delta_{\alpha_k \alpha_j} \ .$$

In the right-hand side of Eq. (2) , $\{\gamma_{\boldsymbol{\alpha}}\}_{1\leq|\boldsymbol{\alpha}|\leq 3}$ and $\{\psi_{\boldsymbol{\alpha}}\}_{1\leq|\boldsymbol{\alpha}|\leq 3}$ are defined as the eigenvalues and the eigeinfunctions of the the integral linear operator $\mathbf{C}$ defined by the kernel $C(\mathbf{x},\mathbf{x}') = \exp(-|x_1 - x_1'|/L)$ in which $L = L_1/40$ and where $\mathbf{x} = (x_1, x_2, x_3)$ and $\mathbf{x}' = (x_1', x_2', x_3')$ belong to $\mathcal{D}$. This means that the correlation length of the random field is much smaller than the length L_1 of the specimen. The eigenvalue problem related to operator $\mathbf{C}$ is then written as

$$\int_{\mathcal{D}} C(\mathbf{x},\mathbf{x}')\psi_{\boldsymbol{\alpha}}(\mathbf{x}')d\mathbf{x}' = \gamma_{\boldsymbol{\alpha}}\psi_{\boldsymbol{\alpha}}(\mathbf{x}) \quad . \tag{3}$$

It should be noted that, $Y(\mathbf{x}) = Y(x_1)$ and consequently, $Y(\mathbf{x})$ is independent of x_2 and x_3. Finally, it is assumed that the Poisson coefficient $\mu = 0.3$ and the mass density $\rho = 2.7 \times 10^3\, Kg/m^3$ are deterministic real constants.

The finite element mesh of the structure is shown in Fig. 1 and consists of 8-node isoparametric 3D solid finite elements. There are $N_d = 1620$ degrees of freedom. Let $\mathbf{Z} = (Z_1, Z_2, Z_3, Z_4)$ be the $\mathbb{R}^4$-valued random variable constituted of the 4 independent random variables in Eq. (2) (the random germ of uncertainties). Let $[K(\mathbf{Z})]$ be the random stiffness matrix with values in the set of all the positive-definite symmetric $(N_d \times N_d)$ real matrices. Let $[M]$ and $[D]$ be the mass and the damping matrices such that $[D] = a\,[M]$ with $a = 10^3\, s^{-1}$. Matrices $[M]$ and $[D]$ are deterministic positive-definite symmetric $(N_d \times N_d)$ real matrices. The $\mathbb{R}^{N_d}$-valued random-frequency-response function $\omega \mapsto \mathbf{U}(\omega)$ related to the nodal displacements is such that

$$[A(\omega;\mathbf{Z})]\mathbf{U}(\omega) = \mathbf{f}(\omega) \quad ,$$

in which $[A(\omega;\mathbf{Z})] = -\omega^2\,[M] + i\,\omega\,[D] + [K(\mathbf{Z})]$ is the dynamic stiffness matrix and where $\mathbf{f}(\omega)$ is the $\mathbb{R}^{\mathbb{N}_d}$-vector of the external forces. Let $\mathbf{U}_\Gamma(\omega)$ be the vector corresponding to the $N_b = 60$ nodes belonging to $\partial\mathcal{D}$ which can be written as $\mathbf{U}_\Gamma(\omega) = \mathbb{P}(\mathbf{U}(\omega))$ in which $\mathbb{P}$ is a linear mapping from $\mathbb{R}^{\mathbb{N}_d}$ into $\mathbb{R}^{\mathbb{N}_b}$. The experimental database is constituted of $m = 100$ realizations of random vector $\mathbf{U}_\Gamma(\omega)$ which are denoted by $\mathbf{u}_\Gamma^1(\omega) = \mathbf{U}_\Gamma(\omega,\theta_1), \ldots, \mathbf{u}_\Gamma^m(\omega) = \mathbf{U}_\Gamma(\omega,\theta_m)$ corresponding to the specimens and for ω running through the frequency band of analysis.

3 Identification of the random field modeling the Young modulus by solving an inverse problem

The finite element approximation $\widetilde{Y}$ of random field Y indexed by $\mathcal{D}$ is written as $\widetilde{Y}(\mathbf{x}) = \sum_{k=1}^{N} R_k h_k(x_1)$ in which $h_1(x_1), \ldots, h_N(x_1)$ are the usual linear interpolation functions related to the finite element mesh of domain $\mathcal{D}$, where $N = 60$ is the degree of this approximation and where $R_1, \ldots R_N$ are the random coefficients. We introduce the $\mathbb{R}^N$-valued random variable $\mathbf{R}$ such that $\mathbf{R} = (R_1, \ldots, R_N)$. Let $[\widetilde{A}(\omega;\mathbf{R})]$ be the random dynamical stiffness matrix constructed by using the finite element approximation $\widetilde{Y}(\mathbf{x})$ of the Young modulus. For each realization $\mathbf{u}_\Gamma^j(\omega)$ belonging to the experimental database, the realization $\mathbf{r}^j = \mathbf{R}(\theta_j)$ of the random variable $\mathbf{R}$ are constructed by solving the nonlinear optimization problem (see [5])

$$\min_{\mathbf{r}^j} \ell_{dyn}(\mathbf{r}^j, \mathbf{u}_\Gamma^j) \quad , \tag{4}$$

in which

$$\ell_{dyn}(\mathbf{r}^j, \mathbf{u}_\Gamma^j) = \sum_{k=1}^{N_{band}} \int_{B_k} \left\| \mathbb{P}\left([\widetilde{A}(\omega;\mathbf{r}^j)]^{-1}\mathbf{f}(\omega)\right) - \mathbf{u}_\Gamma^j(\omega) \right\|^2 d\omega \quad . \tag{5}$$

In the right-hand side of Eq. (5) , $B_k = [\omega_{\min,k}, \omega_{\max,k}]$ with $\omega_{\min,k} = \omega_k - B_{eq,k}/2$ and $\omega_{\max,k} = \omega_k + B_{eq,k}/2$ where $B_{eq,k}$ is an equivalent bandwidth related to the eigenfrequency ω_k of the mean model of the specimens and where N_{band} is the number of bands considered for the identification. It should be noted that the optimization problem introduced in [4] in order to solve the inverse problem to calculate the realizations $\mathbf{r}^1, \ldots, \mathbf{r}^m$ of random vector $\mathbf{R}$ is based on an elastostatic problem. In this case, the experimental database is constituted of static measurements and the optimisation problem is

$$\min_{\mathbf{r}^j} \ell_{stat}(\mathbf{r}^j, \mathbf{u}_\Gamma^j) \quad , \tag{6}$$

in which

$$\ell_{stat}(\mathbf{r}^j, \mathbf{u}_\Gamma^j) = \left\| \mathbb{P}\left([\widetilde{A}(0; \mathbf{r}^j)]^{-1} \mathbf{f}(0) \right) - \mathbf{u}_\Gamma^j(0) \right\|^2 \quad .$$

The optimization problems defined by Eqs. (4) and (6) are solved by using a least-squares estimation of nonlinear parameters (see [6]). Finally, for all $\mathbf{x}$ fixed in $\mathcal{D}$, the realizations $\widetilde{y}^1(\mathbf{x}) = \widetilde{Y}(\mathbf{x}; \theta_1), \ldots, \widetilde{y}^m(\mathbf{x}) = \widetilde{Y}(\mathbf{x}; \theta_m)$ of random variable $\widetilde{Y}(\mathbf{x})$ are constructed by using the relation $\widetilde{y}^j(\mathbf{x}) = \mathbf{h}(x_1)^T \, \mathbf{r}^j$ in which $\mathbf{h}(x_1) = (h_1(x_1), \ldots, h_N(x_1))$. Figure 4 shows the graph of realization $x_1 \mapsto \widetilde{y}^1(\mathbf{x})$ with $x_2 = x_3 = 0$ constructed by solving Eq. (4) ("dynamic inverse problem") and Eq. (6) ("static inverse problem").

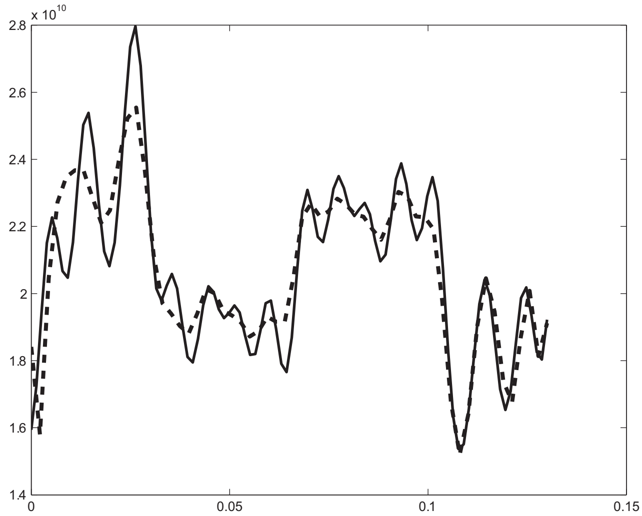

Figure 2: Graph of $x_1 \mapsto Y(\mathbf{x}; \theta_1)$ (thick solid line) and graph of realization $x_1 \mapsto \widetilde{y}^1(\mathbf{x})$ with $x_2 = x_3 = 0$ constructed by solving the "dynamic inverse problem" (dash line) with $N_{band} = 5$. Horizontal axis: x_1. Vertical axis: $Y(\mathbf{x}; \theta_1)$ and $\widetilde{Y}^1(\mathbf{x})$

4 Statistical reduction

The size of the random vector $\mathbf{R}$ can be reduced. Let $\lambda_1 \geq \ldots \geq \lambda_N$ be the eigenvalues of the covariance matrix $[C_{\mathbf{R}}]$ of random vector $\mathbf{R}$. The normalized eigenvectors associated with the eigenvalues $\lambda_1, \ldots, \lambda_N$ are denoted by $\boldsymbol{\varphi}_1, \ldots, \boldsymbol{\varphi}_N$. Consequently, the random vector $\mathbf{R}$ can be written as

$$\mathbf{R} = \underline{\mathbf{R}} + \sum_{k=1}^{N} Q_k \sqrt{\lambda_k} \boldsymbol{\varphi}_k \quad ,$$

in which $Q_1, \ldots, Q_N$ are N centered real-valued random variables defined by $\sqrt{\lambda_k} Q_k = \boldsymbol{\varphi}_k^T (\mathbf{R} - \underline{\mathbf{R}})$ where $\underline{\mathbf{R}} = E\{\mathbf{R}\}$ such that for all k and ℓ, $E\{Q_k\} = 0$ and $E\{Q_k Q_\ell\} = \delta_{k\ell}$. From the study of the function $n \mapsto \sum_{k=1}^{n} \lambda_k$, it can be deduced that random vector $\mathbf{R}$ can be approximated by the random vector $\underline{\mathbf{R}} + [\Phi]\,[\Lambda]\mathbf{Q}^\mu$ with $\mu = 15 < N$ in which the $(\mu \times \mu)$ matrix $[\Lambda]$ and the $(N \times \mu)$ matrix $[\Phi]$ are such that $[\Lambda]_{\ell k} = \delta_{\ell k}\sqrt{\lambda_\ell}$ and $[\Phi]_{\ell k} = [\boldsymbol{\varphi}_k]_\ell$ and where $\mathbf{Q}^\mu = (Q_1, \ldots, Q_\mu)$. For all $j = 1, \ldots, m$, the realization $\mathbf{q}^j = \mathbf{Q}^\mu(\theta_j)$ of random vector $\mathbf{Q}^\mu$ is calculated by $\mathbf{q}^j = [\Lambda]^{-1}[\Phi]^T(\mathbf{r}^j - \underline{\mathbf{R}})$.

5 Chaos decomposition

Let $\mathbf{W}^\nu = (W_1, \ldots, W_\nu)$ be the normalized Gaussian random vector such that $E\{W_i W_j\} = \delta_{ij}$. The truncated Chaos representation of the $\mathbb{R}^\mu$-valued random variable $\mathbf{Q}^\mu$ in terms of $\mathbf{W}^\nu$ is written as

$$\mathbf{Q}^{\mu,\nu} = \sum_{\boldsymbol{\alpha},|\boldsymbol{\alpha}|=1}^{+\infty} \mathbf{a}_{\boldsymbol{\alpha}} H_{\boldsymbol{\alpha}}(\mathbf{W}^\nu) \quad , \tag{7}$$

where $\boldsymbol{\alpha}$ is a multi-index belonging to $\mathbb{N}^\nu$ and where $H_{\boldsymbol{\alpha}}(\mathbf{W}^\nu)$ is the multi-indexed Hermite polynomials (see section 3). The coefficients $\mathbf{a}_{\boldsymbol{\alpha}}$ belonging to $\mathbb{R}^\mu$ are such that $\sum_{\boldsymbol{\alpha},|\boldsymbol{\alpha}|=1}^{+\infty} \mathbf{a}_{\boldsymbol{\alpha}} \mathbf{a}_{\boldsymbol{\alpha}}^T = [I_\mu]$ in which $[I_\mu]$ is the $(\mu \times \mu)$ unit matrix. The truncated Chaos representation of random vector $\mathbf{Q}^{\mu,\nu}$ is denoted by $\mathbf{Q}^{\mu,\nu,d}$ and is such that $\mathbf{Q}^{\mu,\nu,d} = \sum_{\boldsymbol{\alpha},|\boldsymbol{\alpha}|=1}^{d} \mathbf{a}_{\boldsymbol{\alpha}} H_{\boldsymbol{\alpha}}(\mathbf{W}^\nu)$. Consequently, for all $\mathbf{x} \in \mathcal{D}$, the random Young modulus $\widetilde{Y}(\mathbf{x})$ can be approximated by the random variable $\widetilde{Y}^{\mu,\nu,d}(\mathbf{x}) = \mathbf{h}(x_1)^T\,([\Phi]\,[\Lambda]\mathbf{Q}^{\mu,\nu,d} + \underline{\mathbf{R}})$.

The maximum likelihood method (see, for instance, [7]) is used to estimate parameters $\mathbf{a}_{\boldsymbol{\alpha}}$ from realizations $\mathbf{q}^1, \ldots, \mathbf{q}^m$. We then have to solve the following problem of optizimation: find $\mathbb{A} = \{\mathbf{a}_{\boldsymbol{\alpha}}, |\boldsymbol{\alpha}| = 1, \ldots, d\}$ such that

$$\max_{\mathbb{A}} L(\mathbf{q}^1, \ldots, \mathbf{q}^m; \mathbb{A}) \quad , \quad \text{with} \quad \sum_{\boldsymbol{\alpha},|\boldsymbol{\alpha}|=1}^{d} \mathbf{a}_{\boldsymbol{\alpha}} \mathbf{a}_{\boldsymbol{\alpha}}^T = [I_\mu] \tag{8}$$

where $L(\mathbf{q}^1, \ldots, \mathbf{q}^m; \mathbb{A}) = p_{\mathbf{Q}^{\mu,\nu,d}}(\mathbf{q}^1, \mathbb{A}) \times \ldots \times p_{\mathbf{Q}^{\mu,\nu,d}}(\mathbf{q}^m, \mathbb{A})$ is the likelihood function associated with observations $\mathbf{q}^1, \ldots, \mathbf{q}^m$ and where $p_{\mathbf{Q}^{\mu,\nu,d}}$ is the probability density function of $\mathbf{Q}^{\mu,\nu,d}$. However, the optimization problem defined by Eq. (8) yields a very high computational cost induced by the estimation of the joint probability density functions $p_{\mathbf{Q}^{\mu,\nu,d}}(\mathbf{q}^j, \mathbb{A})$ (even for reasonable values of the length μ of random vector $\mathbf{Q}^{\mu,\nu,d}$). Consequently, it is proposed to substitute the usual likelihood function by the pseudo-likelihood function

$$\widetilde{L}(\mathbf{q}^1, \ldots, \mathbf{q}^m; \mathbb{A}) = \prod_{k=1}^{\mu} p_{Q_k^{\mu,\nu,d}}(q_k^1, \mathbb{A}) \times \ldots \times \prod_{k=1}^{\mu} p_{Q_k^{\mu,\nu,d}}(q_k^m, \mathbb{A}) \tag{9}$$

where $\mathbf{q}^j = (q_1^j, \ldots, q_\mu^j)$ and $\mathbf{Q}^{\mu,\nu,d} = (Q_1^{\mu,\nu,d}, \ldots, Q_\mu^{\mu,\nu,d})$ and where $p_{Q_k^{\mu,\nu,d}}$ is the probability density function of random variable $Q_k^{\mu,\nu,d}$. Finally, the following problem of optimization is substituted to the problem defined by Eq. (8) . Find $\mathbb{A} = \{\mathbf{a}_{\boldsymbol{\alpha}}, |\boldsymbol{\alpha}| = 1, \ldots, d\}$ such that

$$\max_{\mathbb{A}} \widetilde{L}(\mathbf{q}^1, \ldots, \mathbf{q}^m; \mathbb{A}) \quad , \quad \text{with} \quad \sum_{\boldsymbol{\alpha},|\boldsymbol{\alpha}|=1}^{d} \mathbf{a}_{\boldsymbol{\alpha}} \mathbf{a}_{\boldsymbol{\alpha}}^T = [I_\mu] \quad . \tag{10}$$

6 Convergence Analysis

In order to perform a convergence analysis of the method proposed in this paper, the normalized random variables $\mathcal{Y}(\mathbf{x})$ and $\widetilde{\mathcal{Y}}^{\mu,\nu,d}(\mathbf{x})$ defined by $\mathcal{Y}(\mathbf{x}) = Y(\mathbf{x})/E\{Y(\mathbf{x})\}$ and $\widetilde{\mathcal{Y}}^{\mu,\nu,d}(\mathbf{x}) = \widetilde{Y}^{\mu,\nu,d}(\mathbf{x})/E\{\widetilde{Y}^{\mu,\nu,d}(\mathbf{x})\}$, for all $\mathbf{x} \in \mathcal{D}$, are introduced. Let $r(\mathbf{x}, \mathbf{x}')$ and $r^{n,\nu,d}(\mathbf{x}, \mathbf{x}')$ be the correlation functions of the random fields $\mathcal{Y}$ and $\widetilde{\mathcal{Y}}^{n,\nu,d}$ such that, for all $\mathbf{x}$ and $\mathbf{x}'$ in $\mathcal{D}$,

$$r(\mathbf{x}, \mathbf{x}') = \frac{E\{\mathcal{Y}(\mathbf{x})\mathcal{Y}(\mathbf{x}')\} - 1}{\sqrt{(E\{\mathcal{Y}(\mathbf{x})^2\} - 1)(E\{\mathcal{Y}(\mathbf{x}')^2\} - 1)}} \quad ,$$

and

$$r^{n,\nu,d}(\mathbf{x}, \mathbf{x}') = \frac{E\{\widetilde{\mathcal{Y}}^{n,\nu,d}(\mathbf{x})\widetilde{\mathcal{Y}}^{n,\nu,d}(\mathbf{x}')\} - 1}{\sqrt{(E\{\widetilde{\mathcal{Y}}^{n,\nu,d}(\mathbf{x})^2\} - 1)(E\{\widetilde{\mathcal{Y}}^{n,\nu,d}(\mathbf{x}')^2\} - 1)}} \quad .$$

The mean-square convergence analysis is performed with respect to the correlation functions and shows that the probabilistic model is converged for $\nu = 4$. The remaining error is due to the truncating of the statistical reduction defined in Section 5.

7 Identification of the probabilistic model

Figure 3 shows the graphs of $\mathbf{x} \mapsto r(\mathbf{x}, \mathbf{x}')$ (thick dashed line) and $\mathbf{x} \mapsto r^{n,\nu,d}(\mathbf{x}, \mathbf{x}')$ (thin solid line) where $\mathbf{x} = (x_1, x_2, x_3)$ and $\mathbf{x}' = (x'_1, x'_2, x'_3)$ with $x_2 = x_3 = 0$ and $x'_1 = 0.0520, x'_2 = x'_3 = 0$ and with $d = 5$, $\mu = 15$, $\nu = 4$.

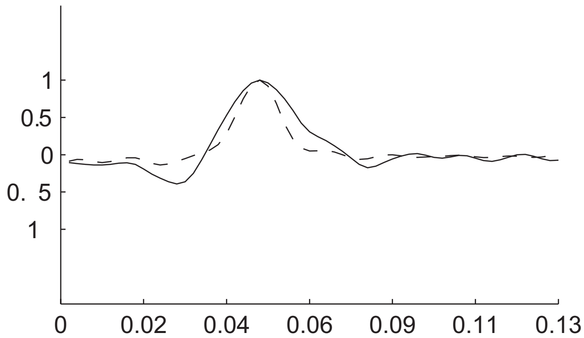

Figure 3: Graphs of $\mathbf{x} \mapsto r(\mathbf{x}, \mathbf{x}')$ (thick dashed line) and $\mathbf{x} \mapsto r^{n,\nu,d}(\mathbf{x}, \mathbf{x}')$ (thin solid line) where $\mathbf{x} = (x_1, x_2, x_3)$ and $\mathbf{x}' = (x'_1, x'_2, x'_3)$ with $x_2 = x_3 = 0$ and $x'_1 = 0.0520, x'_2 = x'_3 = 0$ and with $q = 5$, $\mu = 15$, $\nu = 4$. Horizontal axis: x_1. Vertical axis: $r(\mathbf{x}, \mathbf{x}')$ and $r^{n,\nu,d}(\mathbf{x}, \mathbf{x}')$

For all $\mathbf{x} \in \mathcal{D}$, let $y \mapsto p_{\mathcal{Y}(\mathbf{x})}(y; \mathbf{x})$ and $y \mapsto p_{\widetilde{\mathcal{Y}}^{\mu,\nu,d}(\mathbf{x})}(y; \mathbf{x})$ be the probability density functions of the random variables $\mathcal{Y}(\mathbf{x})$ and $\widetilde{\mathcal{Y}}^{\mu,\nu,d}(\mathbf{x})$. Figure 4 shows the graphs of $y \mapsto \log_{10}(p_{\mathcal{Y}(\mathbf{x})}(y; \mathbf{x}))$ (thick solid line) and $y \mapsto \log_{10}(p_{\widetilde{\mathcal{Y}}^{\mu,\nu,d}(\mathbf{x})}(y; \mathbf{x}))$ (thin solid line) where $\mathbf{x} = (x_1, x_2, x_3)$ with $x_2 = x_3 = 0$ and $x_1 = 0.0152$ with $d = 5$, $\mu = 15$ and $\nu = 4$. It can be seen that the probabily density function is accurately identified.

8 Conclusion

A method for solving the stochastic inverse problem using chaos representation of the stochastic field to be identified and an experimental database is proposed. The proposed method uses the maximum likelihood principle to identify the coefficients of the chaos representation. For presented example, this method allows any probabilistic quantities to be identified such as the autocorrelation function of the random field and the marginal probability density functions. It should be noted that the proposed method can easily be extended to the case of a viscoelastic random medium for which the elastic properties depend on frequency.

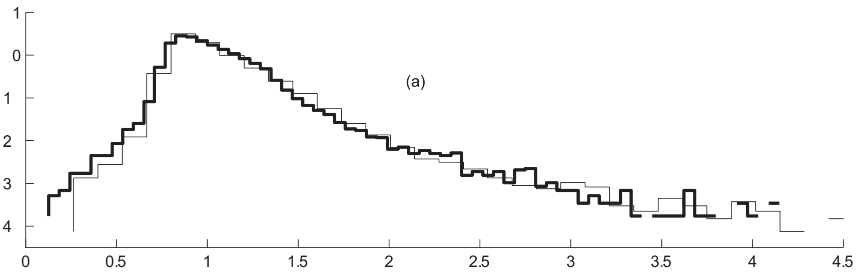

Figure 4: Graphs of $y \mapsto \log_{10}(p_{\mathcal{Y}(\mathbf{x})}(y;\mathbf{x}))$ (thick solid line) and $y \mapsto \log_{10}(p_{\widetilde{\mathcal{Y}}^{\mu,\nu,d}(\mathbf{x})}(y;\mathbf{x}))$ (thin solid line) where $\mathbf{x} = (x_1, x_2, x_3)$ with $x_2 = x_3 = 0$ and $x_1 = 0.0152$ with $d = 5$, $\mu = 15$ and $\nu = 4$. Horizontal axis: y. Vertical axis: $\log_{10}(p_{\mathcal{Y}(\mathbf{x})}(y;\mathbf{x}))$ and $\log_{10}(p_{\widetilde{\mathcal{Y}}^{\mu,\nu,d}(\mathbf{x})}(y;\mathbf{x}))$.

References

[1] Wiener, N., 1938, “The Homogeneous Chaos” , American Journal of Mathematics, **60**: 897-936.

[2] Ghanem, R., and Spanos, P., 1991, “ Stochastic Finite Elements: A Spectral Approach”, Springer-Verlag, New York.

[3] Soize, C., and Ghanem, R., 2004, “Physical Systems with Random Uncertainties: Chaos Representations with Arbitrary Probability Measure”,SIAM Journal of Scientific Computing, 28(2), 395-410

[4] Desceliers, C., and Ghanem, R., and Soize, C., 2004, “ Maximum Likelihood Estimation of Stochastic Chaos Representations from Experimental Data”, International Journal for Numerical Methods in Engineering, 66(6), 978-1001.

[5] Desceliers, C., and Soize, C., and Ghanem, R., 2006, “ Identification of Chaos Representations of Elastic Properties of Random Media using Experimental vibration Tests ”, Computational Mechanics, in press

[6] Marquardt D., 1963, “An Algorithm for Least-squares Estimation of Nonlinear Parameters”, SIAM Journal Applied Mathematics, **11**: 431-441

[7] Serfling, R. J., 1980, “Approximation Theorems of Mathematical Statistics”, John Wiley & Sons.